Biosensors and Bioelectronics 128 (2019) 144–150

Contents lists available at ScienceDirect

Biosensors and Bioelectronics

journal homepage: www.elsevier.com/locate/bios

Highly selective and ultra-sensitive electrochemical sensor behavior of 3D SWCNT-BODIPY hybrid material for eserine detection

Ahmet Şenocak[a], Baybars Köksoy[a], Duygu Akyüz[b], Atıf Koca[b], Darya Klyamer[c,d], Tamara Basova[c,d], Erhan Demirbaş[a], Mahmut Durmuş[a,*]

[a] Department of Chemistry, Gebze Technical University, 41400 Gebze, Kocaeli, Turkey
[b] Department of Chemical Engineering, Marmara University, 34722 Göztepe, Turkey
[c] Nikolaev Institutes of Inorganic Chemistry SB RAS, Lavrentiev Pr. 3, Novosibirsk 630090, Russia
[d] Novosibirsk State University, Pirogova Str. 2, Russia

ARTICLE INFO

Keywords:
Eserine sensor
Pesticide
Click reaction
3D hybrid
BODIPY
SWCNT

ABSTRACT

In this work, 4,4-difluoro-8-(4-hydroxyphenyl) − 2,6-diethynly-1,3,5,7-tetramethyl-4-bora-3a,4a-diaza-*s*-indacene (BODIPY) having double terminal ethynyl groups was synthesized. Three dimensional single walled carbon nanotube (SWCNT)-BODIPY hybrid material (3D SWCNT-BODIPY) was synthesized by the reaction of BODIPY bearing double terminal ethynyl groups with azido containing SWCNTs *via* "Click" reaction. The structural properties and electrochemical detection of eserine (a pesticide) on BODIPY functionalized SWCNTs as a three dimensional (3D) material were investigated. A glassy carbon electrode (GCE) was modified by 3D SWCNT-BODIPY hybrid material for the determination of eserine in the range of 0.25–2.25 μM. In the study by the square wave voltammetry (SWV), the bare GCE showed no response, while the new peak at − 0.6 V appeared in the case of the modified electrode. The detection limit and quantification were determined as 160 nM and 528 nM for eserine on the 3D SWCNT-BODIPY modified electrode, respectively. Eserine was also determined with a standard addition method in different brands of orange juices, and the recovery of eserine was obtained to be in the range of 102.09% and 103.22%. This study clearly indicates that the 3D SWCNT-BODIPY modified electrode tested as an electrochemical sensor was found to be highly selective and sensitive to eserine.

1. Introduction

Every year growing amounts of pesticides and new chemical compounds are used to protect crops, causing undesirable side effects and increase of costs of food production. This also leads to a significant increase of the concentration of pesticides in food and in the environment with associated negative effects on human health (Nsibande, and Forbes, 2016). Moreover, it is now better understood that pesticides have significant adverse effects to health, including cancer, neurological effects, diabetes, respiratory diseases, and genetic disorders. These health effects depend on the degree and type of exposure (Samsidar et al., 2018).

Eserine also known as physostigmine is a highly toxic alkaloid, specifically, a reversible cholinesterase inhibitor. It occurs naturally in the Calabar bean and the Manchineel tree. Eserine is used to treat glaucoma and delays gastric emptying (Potter, 1893). Eserine salicylate is used to treat anticholinergic poisoning because it enhances the transmission of acetylcholine signals in the brain and can cross the blood–brain barrier. Eserine is a drug recommended for pretreatment with the dosage of 30 mg orally twice a day (Balali-Mood and Saber, 2012). At the same time, its overdose can cause cholinergic syndrome as well as it has many side effects like nausea, vomiting, diarrhea, and others. Thus, determination of eserine is very important for human life.

On the other hand, the food chain through soil and water is a critical health hazard to animals and humans due to the increased use of pesticides (Sassolas et al., 2012). Up to now several techniques are used for the effective detection of pesticides in food and water, *e.g.* enzyme-linked immunosorbent assays (ELISAs) (Nunes et al., 1998), liquid chromatography-mass spectroscopy (LC-MS) (Stachniuk and Fornal, 2016), gas chromatography mass spectroscopy (GC-MS) (Michel and Buszewski, 2002) and high-performance liquid chromatography (HPLC) (Metwally et al., 1997). However, the methods mentioned above are expensive and require trained staff. Therefore, it is necessary to develop novel techniques and modern strategies for the detection of pesticides, which are rapid, selective, reliable, low cost, and sensitive (Aragay et al., 2012). In this connection, electrochemical techniques can be a

* Corresponding author.
E-mail address: durmus@gtu.edu.tr (M. Durmuş).

https://doi.org/10.1016/j.bios.2018.12.052
Received 12 October 2018; Received in revised form 15 December 2018; Accepted 28 December 2018
Available online 09 January 2019
0956-5663/

promising alternative due to their specificity, response rate, wide applicability and mass production (Smith et al., 2008).

In the last years, electrochemical sensors become the most popular ones for the detection of various chemical and biochemical compounds (Zhu et al., 2015). Carbon nanotubes (CNTs) and in particular single walled carbon nanotubes (SWCNTs) are very promising materials for sensing applications due to their attractive electronic structure (Balasubramanian and Burghard, 2006; Polyakov et al., 2017). Moreover, CNTs have some fascinating advantages in producing electrochemical sensors and biosensors with excellent properties, *e.g.* small size, high surface area, superior biocompatibility, good conductivity, convertible sidewall, and high reactivity (Rivas et al., 2007). In addition, chemical functionalization of CNTs is used to bind desired chemical groups, which can provide their improved biocompatibility and solubility. Preparation of fine CNT dispersions makes it possible the creation of various composite electrodes. Recently CNT-based 3D architecture has attracted attention of some research groups (Ajayan and Zhou, 2001; Romo-Herrera et al., 2007; Terao, 2009; Şenocak et al., 2018a, 2018b, 2018c), because 3D structures with their bigger cavities and higher surface area possess all properties important for sensing application. For instance, 3D SWCNT hybrid materials were shown in our previous works (Şenocak et al., 2018a, 2018b, 2018c) to be promising sensors with stability, selectivity and very low detection limit both for detection of gaseous ammonia and for determination of quercetin in aqueous media.

BODIPY molecules show remarkable photophysical properties such as excellent photostability, high fluorescence quantum yield and high molar extinction coefficient of absorbance. BODIPY derivatives have superior performance as functional dyes applied in solar cell devices (Bessette, and Hanan, 2014), organic light-emitting diodes (Ni and Wu, 2014), bioprobes (Yao et al., 2013), chemosensors (Boens et al., 2012) and photodynamic therapy (Göl et al., 2014).

In this study, a sensitive, rapid, simple and selective electrochemical method was developed for the determination of eserine in both aqueous solutions and real samples using 3D SWCNT-BODIPY hybrid. SWCNTs containing azido groups were modified with 4,4-difluoro-8-(4-hydroxyphenyl)-2,6-diethynly-1,3,5,7-tetramethyl-4-bora-3a,4a-diaza-s-indacene (BODIPY) bearing terminal ethynyl groups. The structure of BODIPY derivative was confirmed by ^{1}H NMR, ^{19}F NMR, ^{11}B NMR, ^{13}C NMR, FT-IR, UV–Visible spectroscopies and MALDI-TOF mass spectrometry as well as by elemental analysis. On the other hand, the 3D SWCNT-BODIPY hybrid material was characterized by UV–Visible, Raman and FT-IR spectroscopies and thermogravimetric analysis. The morphology of 3D hybrid material was examined using scanning electron (SEM) and transmission electron (TEM) microscopies. Square wave voltammetry (SWV) was used to evaluate the electrochemical sensor response of the 3D hybrid material towards eserine in aqueous solutions and real samples.

2. Materials and methods

The synthesis of the BODIPY and used materials/equipment were supplied in the Supplementary Information.

2.1. Preparation of 3D SWCNT-BODIPY hybrid material

4 mg of SWCNT-N_3 was added to 3 mL of DMF as a suspension and sonicated for 30 min. 20 mg (0.052 mmol) of BODIPY was dissolved in 2 mL DMF. The BODIPY solution was added to the SWCNT-N_3 suspension drop wise. 0.90 mg (0.0045 mmol) of sodium L-ascorbate and 0.225 mg (0.0009 mmol) of copper(II) sulfate pentahydrate were added to the mixture as catalysts and the reaction mixture was left at 85 °C for 24 h. Finally, the reaction mixture was filtered and washed with water, ethanol and acetone sequentially and dried in nitrogen atmosphere (Scheme 1). FTIR ν (cm^{-1}): 3280 (CH of triazole ring), 3060 (Ar-CH), 2984–2843 (Aliphatic CH), 1606-1518 (C=C), 1478 (B-N), 1175 (Ar C=C).

2.2. GCE modification with 3D SWCNT-BODIPY hybrid material

The bare GCE was cleaned with 1.0, 0.3 and 0.05 μm alumina slurries to obtain a polished surface, washed with ultra-pure distilled water and dried in oven at 60 °C. 1 mg/mL hybrid solution was prepared in DMF and ultrasonicated for 20 min at 25 °C. Different amount of hybrid suspension such as 5, 7 and 10 μL was dropped onto GCE surface and dried at 60 °C in oven for half an hour. After the tests of different volumes of the prepared hybrid solution, a drop of 10 μL was chosen as an optimal one due to the good shape of peaks. The modified electrode was designated as 3D SWCNT-BODIPY/GCE.

2.3. Real samples assay procedure

Different brands of orange juice samples were purchased from a local market. After 15 min of ultrasonication, 1.0 mL of the real sample was added to 3.0 mL PBS (a pH of 7.0). Then, the SWV measurements from −1.0 to + 1.0 V were performed for the determination of eserine concentration in the solution. SWV measurements were carried out at 25 °C. Each measurement was repeated 3 times and average values were taken.

3. Results and discussion

3.1. Characterization of the BODIPY and its 3D SWCNT-BODIPY hybrid material

Three characteristic vibrations at 3485 cm^{-1} for -OH, 3297–3277 cm^{-1} for -C≡C-H and 2111 cm^{-1} for -C≡C- groups are observed in the FTIR spectra of BODIPY derivative (Fig S1a). Moreover, as seen on the ^{1}H NMR spectrum of BODIPY (**3**), the aromatic ring protons were monitored as doublets between 7.38 and 6.98 ppm. The hydroxyl proton was observed as a broad peak at 5.45 ppm (Fig S2). Methyl protons of BODIPY were observed as singlets at 1.55 and 2.65 ppm and other proton belonging to ethynyl groups were observed as a singlet at 3.32 ppm. Also the carbon skeleton of **3** was confirmed by ^{13}C NMR spectrum (Fig S3). Only one boron atom in the BODIPY core was assigned at 0.52 ppm as a triplet in the ^{11}B NMR spectrum (Fig S4) due to the NMR active neighbor fluorine atoms and these atoms were monitored as doublets at −146.5 and −146.3 ppm in the ^{19}F NMR spectrum of compound **3** (Fig S5). Additionally, the structure of BODIPY compound was confirmed by the MALDI-TOF mass spectrum exhibiting the molecular ion peak $[M]^+$ at 388.525 *m/z* (Fig S6).

FTIR spectra of diethynyl BODIPY, SWCNT-N_3 and 3D SWCNT-BODIPY hybrid are shown in Fig. S1a. The BODIPY compound exhibits the vibration peaks at 3297–3277 and 2111 cm^{-1} attributed to H-C≡C- and R-C≡C-R stretching vibrations, respectively. In addition, the vibrations of N_3 groups in SWCNT-N_3 were observed at 2106 cm^{-1}. The ethynyl peaks of BODIPY derivative and the azide peak of SWCNTs-N_3 disappeared when the 3D SWCNT-BODIPY hybrid formed (Fig. S1a). The appearance of stretching vibrations of -CH in triazole ring at 3280 cm^{-1} additionally testified that the "*Click*" reaction was occurred. Moreover, a small peak corresponding to azide vibration was still observed in the FTIR spectrum of 3D SWCNT-BODIPY hybrid material due to the rest of some unreacted azide groups.

3D SWCNT-BODIPY hybrid material formed fine dispersion in DMF solution after chemical functionalization of SWCNT with BODIPY. The UV–Vis spectra of 3D hybrid and BODIPY material are presented in Fig. S1b for comparison. The spectrum of BODIPY shows the absorption band at 539 nm, while the 3D hybrid exhibits the broad peak with the absorption maximum at 527 nm which is shifted to the lower wavelengths compared to the band in the BODIPY spectrum. This shift can also indicate strong interaction between SWCNTs and BODIPY.

The Raman spectra of 3D SWCNT-BODIPY hybrid and pristine

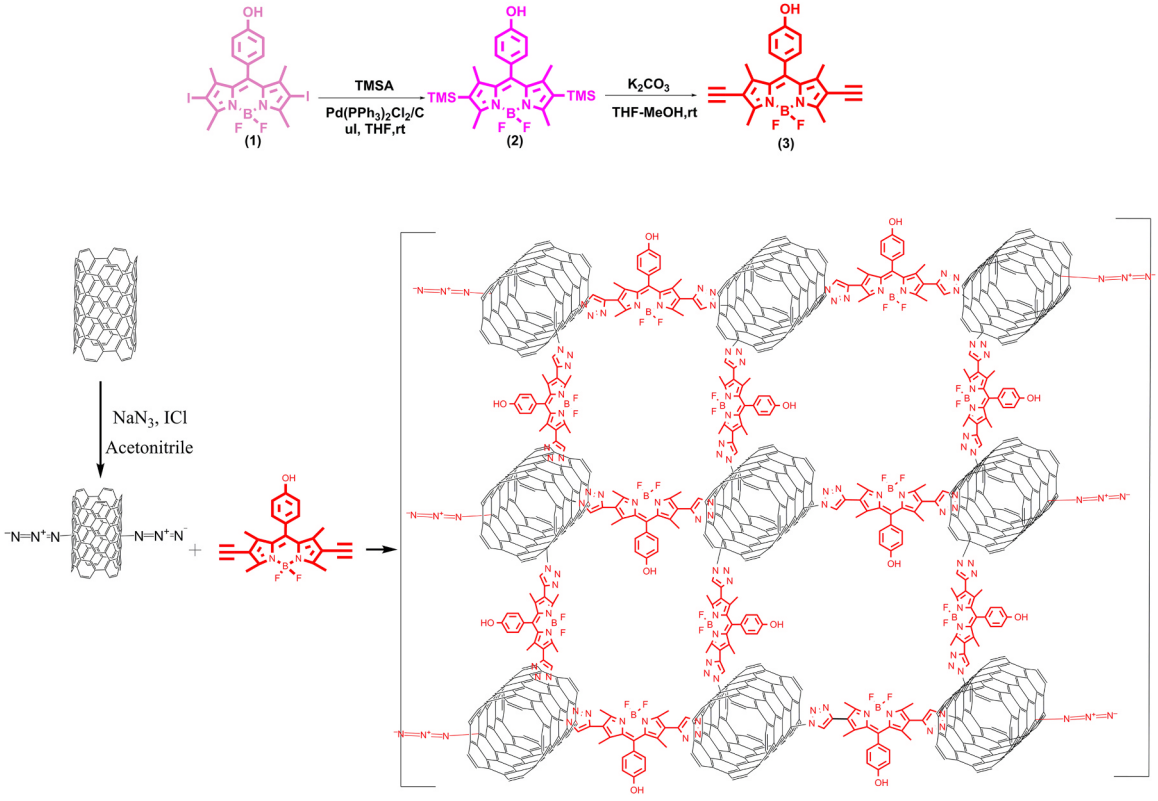

Scheme 1. Synthetic pathway of double terminal ethynyl BODIPY derivative and schematic illustration of the preparation of 3D SWCNT-BODIPY hybrid material.

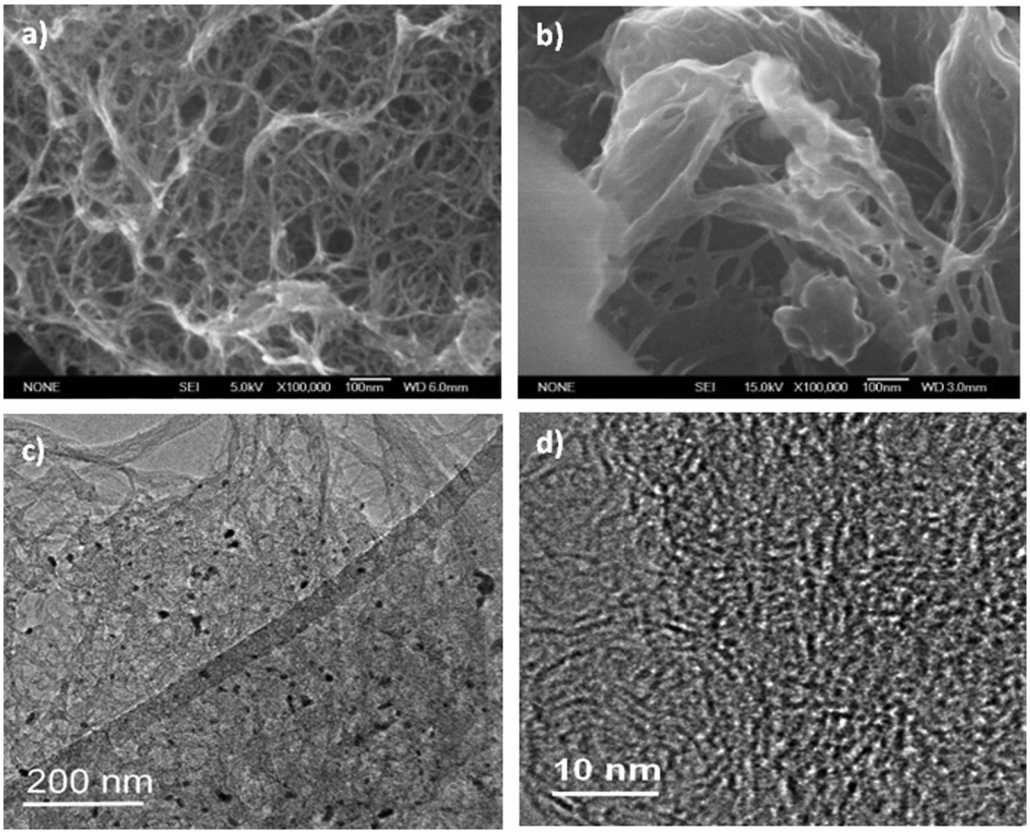

Fig. 1. SEM (a, b) and TEM (c, d) images of 3D SWCNT-BODIPY hybrid.

SWCNT are given in Fig. S7a. The ratio of intensities of disorder (D) mode and graphite mode (G) as well as the radial breathing modes (RBM) are usually compared to exhibit functionalization of carbon nanomaterials (Wepasnick et al., 2010; Alvarez et al., 2001). There are three characteristic groups of modes in the spectrum of pristine SWCNT, namely D mode at 1344 cm^{-1}, G band at 1590 cm^{-1} and RBMs mode in the range of 158–304 cm^{-1}. In the spectrum of 3D SWCNT-BODIPY hybrid the D and G modes shift to 1338 cm^{-1} and 1587 cm^{-1}, respectively. Some characteristic vibrations at 572, 845, 975, 1010, and 1175 cm^{-1} belonging to BODIPY are also observed in the spectrum of 3D SWCNT-BODIPY hybrid. The I_D/I_G ratio in the spectrum of pure SWCNT has a value of 0.045, while this value increases to 0.067 in the 3D SWCNT-BODIPY hybrid spectrum. The RBMs in the range of 158–304 cm^{-1} (Fig. S7a) correspond to a distribution of SWCNT diameters in the range of 0.7–1.4 nm. In the spectrum of 3D SWCNT-BODIPY hybrid the intensities of RBMs noticeably decrease. All these changes clearly denote the functionalization of carbon nanotubes by BODIPY molecules

The amount of BODIPY molecules covalently bonded to SWCNTs was calculated using TGA data **(**Fig. S7b**).** The weight losses of BODIPY, pristine SWCNT, SWCNT-N_3, and 3D SWCNT-BODIPY at 700 °C were 41.64%, 4.42%, 10.44% and 22.65%, respectively. The weight losses of SWCNTs between 200 °C and 700 °C can be explained by the elimination of residual amorphous carbon in SWCNT. The weight losses due to functional chemical groups in SWCNT were determined as 6.02% for SWCNTs-N_3 and 28.60% for 3D SWCNT-BODIPY. The number of azide functional groups in SWCNT-N_3 was calculated as described in the literature (Şenocak et al., 2018a, 2018b, 2018c) to be 1 per 55 carbon atoms. The weight loss due to covalently bonded BODIPY molecules in 3D hybrid was 28.60% (11.91%/41.64%). The amount of BODIPY was estimated as 1 BODIPY molecule per 81 carbon atoms in the 3D SWCNT-BODIPY hybrid according to the calculations (71.40% x388.525)/(28.60%x12).

The morphology of 3D SWCNT-BODIPY hybrid was examined by SEM and TEM **(**Fig. 1**).** As shown in Fig. 1**(a, b),** SEM images of 3D SWCNT-BODIPY hybrid exhibited cross-linked three dimensional porous structures that can be useful for sensing application. TEM images of 3D SWCNT-BODIPY **(**Fig. 1**(c, d))** proved this porous assembly of cross-linked carbon nanotubes. The magnified HR-TEM image shows the cross-linked nanotubes with pores of 1–2 nm in diameter which can trap the pesticide molecule.

3.2. Electrochemical sensor properties of 3D SWCNT-BODIPY material to eserine

Fig. 2 illustrates a fabrication procedure of the sensor based on the investigated 3D hybrid. The modified electrodes 3D SWCNT-BODIPY/GCE were produced by drop casting of different volumes (5, 7 or 10 µL) of the 1 mg/mL hybrid suspension in DMF. After the tests of different volumes, 10 µL aliquot was shown to be optimal due to the better shape of peaks on voltammetric curves.

To demonstrate the applicability of the hybrid material for pesticide detection, the voltammetric behavior of 2 µM pesticides was examined with bare GCE and 3D SWCNT-BODIPY/GCE in PBS (pH = 7) by a square wave voltammetric method. 3D SWCNT-BODIPY/GCE was stabilized with 20 forward and 20 backward measurements between −1 and + 1 V. When 3D SWCNT-BODIPY/GCE was immersed into eserine solution, the new peak appeared around 0.6 V and the peak of 3D hybrid was decreased with eserine addition around −0.0 V (Fig. 3). The oxidation of eserine was easier on 3D SWCNT-BODIPY/GCE in comparison with the bare GCE. Thus, it can be deduced that the surface of 3D SWCNT-BODIPY/GCE plays the role of catalyst in eserine oxidation.

SEM was used for monitoring of the surface morphology of GCE modified with 3D SWCNT-BODIPY hybrid. Fig. S8 represents SEM images of the surface of modified electrode. The modified electrode shows the network structure of randomly distributed flower-like stacks.

3.3. Analytical performance of 3D SWCNT-BODIPY sensor to eserine

SWV is a widely applicable electrochemical method used for various analytical measurements. Fig. 3 illustrates the SWVs of different concentrations of eserine on 3D SWCNT-BODIPY/GCE in 0.1 M PBS with pH = 7.0. The current peak intensity increased linearly with the increase of eserine concentrations in the range from 0.25 to 2.25 µM **(**Fig. 3**).** The detection (LOD) and quantification (LOQ) limits of eserine were found 160 nM and 528 nM (R^2 = 0.997), respectively. In addition to SWV measurements the chronoamperometric method was used to test selectivity and sensitivity of sensors at different concentrations of eserine on 3D SWCNT-BODIPY/GCE in 0.1 M PBS with pH = 7.0 at constant 0.65 V using RRDE. The current response increased linearly with the increase of eserine concentrations in the range from 0.25 to 1.25 µM (Fig. S11a). The detection (LOD) and quantification (LOQ) limits of eserine were found 185 nM and 610.5 nM (R^2 = 0.9994), respectively.

The works on the determination of eserine are only sporadic in the literature and most of them do not deal with its detection in the real samples (Akyüz et al., 2017; Ipek et al., 2015, 2014; Özen et al., 2016; Keleş et al., 2017). The results for eserine detection, obtained in this work are compared with the data reported in the literature using different modified electrodes given in Table 1. According to this table, the newly developed sensor is a superior platform for eserine detection. The prepared 3D SWCNT-BODIPY/GCE possesses the lower LOD, higher

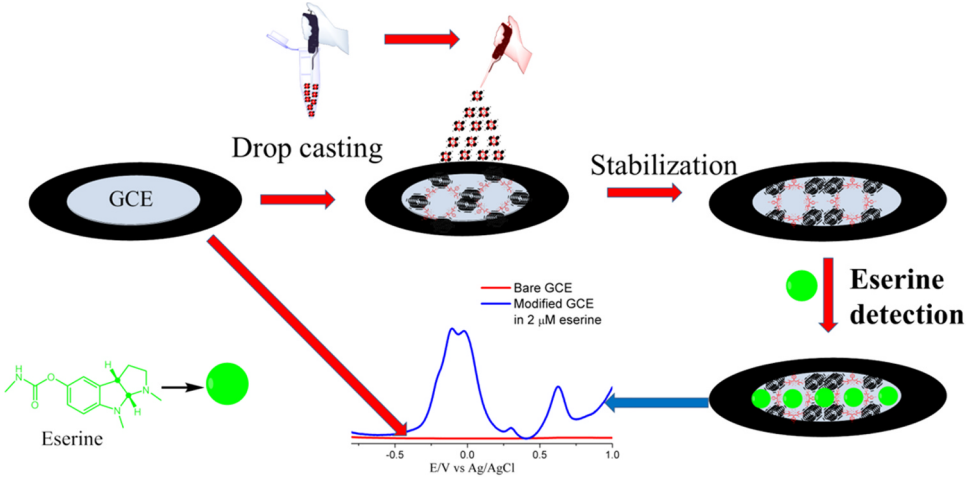

Fig. 2. Schematic illustration of the eserine sensor fabrication.

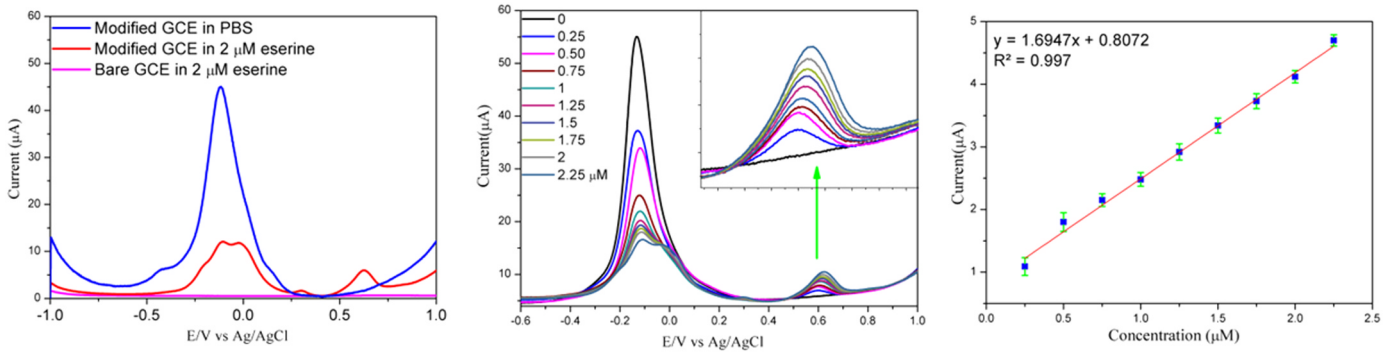

Fig. 3. SWV response of 2 μM of eserine in PBS (pH 7) and SWV calibration graph of eserine on 3D SWCNT-BODIPY/GCE including error bars obtained by relative standard deviations (RSD).

Table 1
Comparison of some voltammetric techniques for the determination of eserine using SWV.

Working electrode	LOD (nM)	Sample	References
GCE/TiOPc	183	seawater	(Akyüz et al., 2017)
GCE/MnClPc	643	seawater	(Akyüz et al., 2017)
GCE/CoPc	10.3	seawater	(Akyüz et al., 2017)
ITO/CoPc-AQ	165	–	(Ipek et al., 2015)
ITO/CoPc-AQ-nPt	469	–	(Ipek et al., 2015)
ITO/CoPc-AQ-nAu	174	–	(Ipek et al., 2015)
GCE/TiOPc	135	–	(Özen et al., 2016)
GCE/MnPc(MOR-NAF)	340	–	(Keleş et al., 2017)
GCE/PANI-N3/TA-CoPc	175	–	(Ipek et al., 2014).
3D SWCNT-BODIPY/GCE	160	Orange juice	**This work**

*AQ: Anthraquinone.
*MOR-NAF: 5-{[(1*E*)-(4-morpholin-4-ylphenyl) methylene]amino}-1-naphthoxy.
*TA: terminal-alkynyl.

selectivity and clearer peak shapes as well as it allows to perform the measurements in the wider concentration range (Table 1). In the most studies, phthalocyanine-based sensors for eserine detection were obtained *via* electropolymerization on different electrodes such as ITO, platinum, gold and GCE (Akyüz et al., 2017; Ipek et al., 2015, 2014; Özen et al., 2016; Keleş et al., 2017). It is worth mentioning that platinum and gold electrodes are quite expensive. At the same time, GCE is inexpensive, easily reusable and widely used for sensing applications. On the other side, SWCNT modification performed in this study was established on easy preparation of 3D SWCNT-BODIPY *via* "*Click*" chemistry and has some advantages compared to the modification techniques based on the treatment by strong acids such as HNO_3 and H_2SO_4 which can damage the surface of SWCNT and disturb their electronic structure. The approach based on "*Click*" reactions allows to obtain porous structures with the highly developed surface and to minimize structural defects on SWCNT surface. This may ensure the good sensing characteristics of 3D SWCNT-BODIPY/GCE given in Table 1. The great performance of 3D SWCNT-BODIPY hybrid films can also be supported by the synergistic electrocatalytic influence of GCE.

To study the sensor selectivity, 3D SWCNT-BODIPY/GCE electrode was tested with various pesticides illustrated in Fig S9. Concerning eserine determination, a gradual increase and decrease of the response at the potentials of 0.60 and −0.13 V were observed in Fig. 3b. This could be related to spontaneous reactivation of hydroxyl groups of 3D SWCNT-BODIPY during the titration combined with the effect of N-containing and aromatic groups in eserine. It was shown that the sensing electrode interacts only with eserine since the developed sensor was sensitive to eserine not other studied pesticides due to having dissimilar molecular structures (Fig S9). Organophosphorus pesticides such as parathion, diazinon, chlorpyrifos methyl and fenitrothion have functional phosphorus and aromatic groups. Methomyl does not contain aromatic ring in contrast to the other tested analytes, and contains amino, carboxyl and sulfur groups. Eserine has functional amino, carboxyl groups and aromatic ring. A two-step detection mechanism can be suggested. On the first step, all six pesticides interact with the functionalized 3D SWCNT-BODIPY *via* non-covalent interaction: organophosphorus pesticides primarily attach the hybrid *via* π-π stacking interaction, methomyl bearing amino and carboxyl groups forms hydrogen bonds while eserine forms both types of contacts with the hybrid material (Hüffer et al., 2017). Thus, the peak at −0.13 V is related only to 3D SWCNT-BODIPY. It decreases slightly upon addition of all pesticides with the exception of eserine while the addition of eserine leads to a sharp decrease of this peak and appearance of a shoulder peak at around 0 V. (Fig. 4c). The second step is connected with the formation of the peak at 0.60 V which appears only in the presence of eserine. The proposed mechanism is also similar to the enzymatic mechanism described by Zhou et al. (2010), Fuxreiter and Warshel (1998) and Zhang et al. (2002). Acetylcholinesterase in enzymatic reaction the 3D hybrid plays the role of a catalyst. In this process, the hydroxyl O atom of BODIPY attacks the carbonyl C atom of eserine resulting in the proton transfer from hydroxyl group to triazole ring of 3D hybrid (Fig S10). The proton transfers to the leaving group of eserine, and the scissile bond breaks with the formation of amide group of eserine metabolite covalently bonded to the 3D hybrid. Note that the peak at 0.60 V is not observed in the case of methomyl bearing a similar amide group but not containing any aromatic rings. This makes the break of the bond between amide and oxygen impossible.

3.4. Stability, reproducibility and selectivity of the pesticide sensor

The mixtures of eserine with various pesticides such as parathion, fenitrothion, methomyl, chlorptrifos methyl and diazinon in the concentration ratio 1:1 (eserine:another interfering pesticide) were studied to test the sensor selectivity. SWV method was used to monitor the peak current of eserine oxidation process in the presence of each interfering pesticide. Before addition of an interfering pesticide, 1 μM eserine was added to the buffer solution and measured by a SWV method. Then the interfering pesticide was added to the buffer solution with eserine. Fig. 4**a** shows that no changes of the peak current were observed in the presence of interfering pesticides. As seen in Fig. 4**a** and **b**, the differences between the peak current of eserine itself and eserine in the presence of interfering pesticides on 3D BODIPY-SWCNT/GCE was no more than 2%, which showed that the prepared sensor exhibits quite good selective for the detection of eserine.

In addition, another interference study was performed in the reverse order. The interfering pesticides were added to the buffer solution without eserine and measured by SWV in order to reveal any interaction occurring on the electrode **(**Fig. 4**c).** No interaction and no peaks on SWV curves (Fig. 4c) were observed in the case of all investigated pesticides in PBS solution. The peak potential of eserine was recorded at

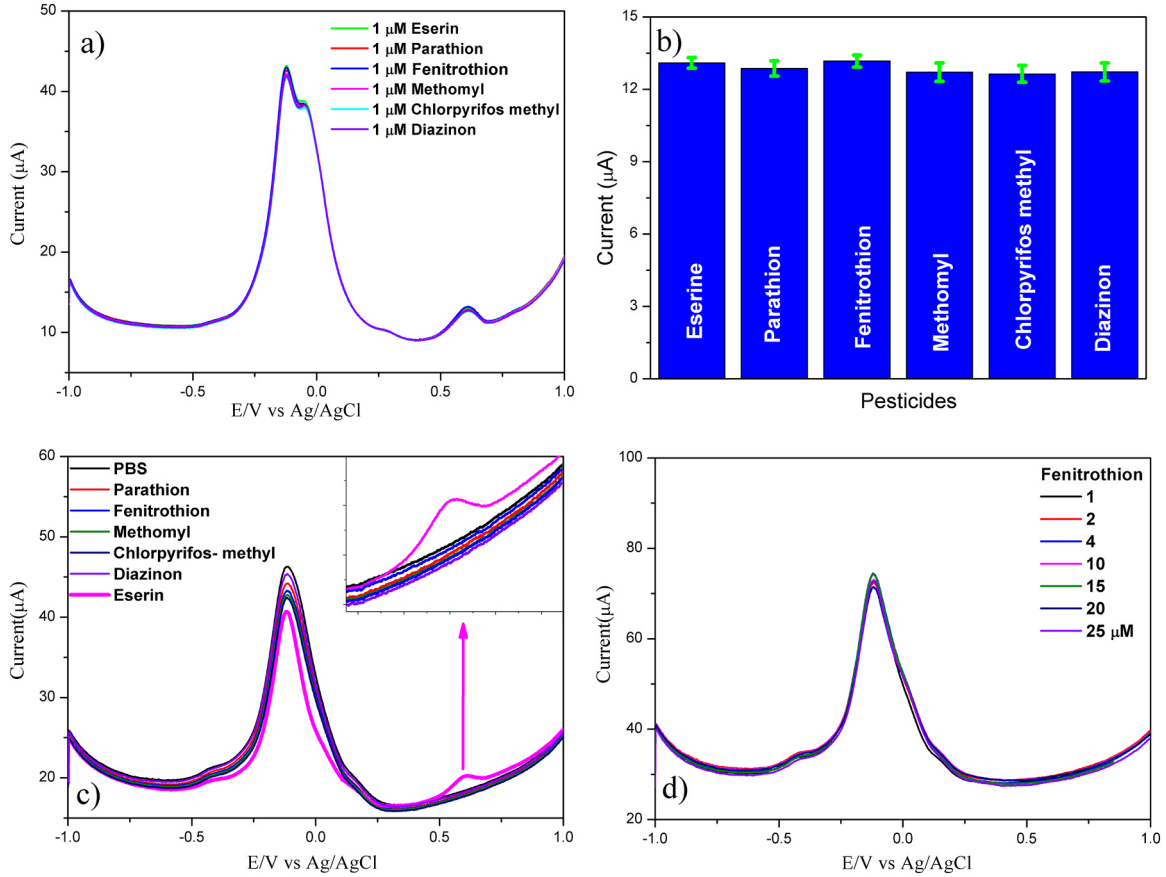

Fig. 4. Selectivity of the sensor: **a)** 1.0 μM of parathion, fenitrothion, methomyl, chlorptrifos methyl and diazinon titration in the presence of 1.0 μM of eserine **b)** a column diagram for peak current responses of (a) including error bars obtained by RSD **c)** 1.0 μM of parathion, fenitrothion, methomly, chlorptrifos methyl and diazinon titration in the absence of 1.0 μM of eserine **d)** fenitrothion pesticide titration recorded on 3D SWCNT-BODIPY/GCE.

600 mV; therefore, the other pesticides did hardly affect the eserine detection. On the other hand, fenitrothion pesticide titration presented in Fig. 4**d** showed no effect on the 3D SWCNT-BODIPY/GCE sensor. In addition, chronoamperometric selectivity test has been performed to support the proposed hypothesis. When the constant voltage of 0.65 V was applied, no changes were observed upon the addition of parathion, fenitrothion, methomyl, chlorpyrifos methyl and diazinon. However, a current increase was observed as eserine was added (Fig S11). It is worth mentioning that the chronoamperometric and voltammetric measurements were in a good agreement with the suggested detection mechanism.

The short-term operational stability and lifetime of the sensor are required for the continuously monitoring of eserine. During the experiment, 10 sequential measurements were carried out in PBS (pH = 7.0) contained 2.5 μM eserine on 3D SWCNT-BODIPY/GCE. After every measurement the electrode was washed with ultra-pure water and then the electrode was immersed into the same solution and measured again. The relative standard deviation was 4.4%, indicating that the electrode modified with 3D SWCNT-BODIPY hybrid was stable. On the other hand, the long-term stability was examined by measuring 2.5 μM eserine solutions intermittently in the course of several weeks. The peak current of eserine oxidation showed only 5.4% decrease compared to the initial peak value after storage of the modified electrode at 25 °C for 4 weeks, indicating high stability of the eserine sensor. Additionally, chronoamperometric technique was used to test the short term stability and reproducibility of the response to eserine. To test the sensor stability five sequential measurements were carried out in PBS (pH = 7.0) contained 2.5 μM eserine on 3D SWCNT-BODIPY/GCE using RRDE (constant potential and rotation speed were 0.65 V and 1000 rpm, respectively). The standard deviation of peak current increments was 5.1%. To test the reproducibility five parallel chronoamperometric measurements were carried out. RSD of peak current increments was 3.8% in every first scan.

3.5. Determination of eserine in orange juice samples on the modified electrode by SWV

Determination of eserine using the 3D-SWCNT-BODIPY hybrid sensor was performed in different orange juice samples by means of a standard addition method. For this purpose, 1 mL of an orange juice sample was added to the investigated solutions for the determination of eserine. The data in Table S1 showed that the prepared sensor had good performance in real samples for determination of eserine. Each measurement was repeated three times and the relative standard deviation was estimated to be less than 5%, indicating its high accuracy. Recovery of eserine was estimated for the determination of sensor efficiency. The recovery was found to be between 102.09% and 103.22%, showing reliability and efficiency of this method.

4. Conclusions

A glassy carbon electrode modified by 3D SWCNT-BODIPY hybrid material for the determination of low concentrations of eserine for the first time was evaluated by square wave voltammetric and chronoamperometric methods. The linear range, detection and quantification limits of eserine were 0.25–2.25 μM, 160 and 528 nM, respectively. All six pesticides interacted with the functionalized 3D SWCNT-BODIPY *via* non-covalent interaction. The peak at −0.13 V was corresponded to 3D SWCNT-BODIPY. The other one related to the formation of peak at 0.60 V was confirmed for the presence of eserine in PBS. This work

created new prospects for the application of non-enzymatic sensors for the selective detection of pesticides *via* an enzymatic-like mechanism. It indicated that the obtained non-enzymatic sensor exhibited the superior selectivity, high sensitivity and great stability of the sensor responses to eserine in both water and in real samples. Furthermore, this work can be expanded on to fabricate of this sensor in the future and the price is assumed approximately 0.2 $.

CRediT author statement

Ahmet Şenocak synthesized 3D hybrid material, performed its characterization, carried out the electrochemical sensor experiment, analysed the data and wrote the manuscript. **Baybars Köksoy** synthesized BODIPY and performed its characterization. **Duygu Akyüz** helped in sensor measurements. **Atıf Koca** provided guidance during the sensor research process. **Darya Klyamer** carried out TEM and Raman characterization. **Tamara Basova** carried out TEM and Raman characterization and also checked the manuscript. **Erhan Demirbaş** analysed the data checked the manuscript and supervised the project. **Mahmut Durmuş** conceived the original idea and provided theoretical guidance during the research process. All co-authors reviewed and approved the manuscript.

Declaration of interests

None.

Appendix A. Supplementary material

Supplementary data associated with this article can be found in the online version at https://doi.org/10.1016/j.bios.2018.12.052.

References

Ajayan, P.M., Zhou, O.Z., 2001. Top. Appl. Phys. 80, 391–425.
Akyüz, D., Keleş, T., Biyiklioglu, Z., Koca, A., 2017. Electroanal 29, 2913–2924.
Alvarez, L., De la Fuente, G., Righi, A., Rols, S., Anglaret, E., Sauvajol, J., Munoz, E., Maser, W., Benito, A., Martinez, M., 2001. Phys. Rev. B 63, 153401.
Aragay, G., Pino, F., Merkoçi, A., 2012. Chem. Rev. 112, 5317–5338.
Balali-Mood, M., Saber, H., 2012. Iran. J. Med. Sci. 37, 74–91.
Balasubramanian, K., Burghard, M., 2006. Anal. Bioanal. Chem. 385, 452–468.
Bessette, A., Hanan, G.S., 2014. Chem. Soc. Rev. 43, 3342–3405.
Boens, N., Leen, V., Dehaen, W., 2012. Chem. Soc. Rev. 41, 1130–1172.
Fuxreiter, M., Warshel, A., 1998. J. Am. Chem. Soc. 120, 183–194.
Göl, C., Malkoç, M., Yeşilot, S., Durmuş, M., 2014. Dalton Trans. 43, 7561–7569.
Hüffer, T., Sun, H., Kubicki, J.D., Hofmann, T., Kah, M., 2017. Environ. Sci. Nano 4, 1045–1053.
Ipek, Y., Dinçer, H., Koca, A., 2014. J. Electrochem Soc. 161, B183–B190.
Ipek, Y., Şener, M.K., Koca, A., 2015. J. Porphyr. Phthalocyanines 19, 1–11.
Keleş, T., Akyüz, D., Biyiklioglu, Z., Koca, A., 2017. Electroanalysis 29, 2125–2137.
Metwally, M.E.S., Osman, M.S., Al-Rushaid, R., 1997. Food Chem. 59, 283–290.
Michel, M., Buszewski, B., 2002. 25, 2293–2306.
Ni, Y., Wu, J., 2014. Org. Biomol. Chem. 12, 3774–3791.
Nsibande, S.A., Forbes, P.B.C., 2016. Anal. Chim. Acta 945, 9–22.
Nunes, G.S., Toscano, I.A., Barcelo, D., 1998. Trends Anal. Chem. 17, 79–87.
Özen, Ü.E., Keleş, T., Bıyıklıoğlu, Z., Koca, A., Özkaya, A.R., 2016. J. Electrochem Soc. 163, B673–B682.
Polyakov, M.S., Basova, T.V., Göksel, M., Şenocak, A., Demirbaş, E., Durmuş, M., Kadem, B., Hassan, A., 2017. Synth. Met. 227, 78–86.
Potter, S.O.L., 1893. A Handbook of Materia Medica, Pharmacy and Therapeutics. P. Blakiston Son & Co, London, pp. 293.
Rivas, G.A., Rubianes, M.D., Rodríguez, M.C., Ferreyra, N.F., Luque, G.L., Pedano, M.L., Miscoria, S.A., Parrado, C., 2007. Talanta 74, 291–307.
Romo-Herrera, J.M., Terrones, M., Terrones, H., Dag, S., Meunier, V., 2007. Nano Lett. 7, 570–576.
Samsidar, A., Siddiquee, S., Shaarani, S., 2018. Trends Food Sci. Technol. 71, 188–201.
Sassolas, A., Prieto-Simon, B., Marty, J.L., 2012. Am. J. Anal. Chem. 3, 210–232.
Şenocak, A., Göl, C., Basova, T.V., Demirbaş, E., Durmuş, M., Al-Sagur, H., Kadem, B., Hassan, A., 2018a. Sens. Actuators B 256, 853–860.
Şenocak, A., Kaya, E.N., Kadem, B.Y., Basova, T.V., Demirbaş, E., Hassan, A.K., Durmuş, M., 2018b. Dalton Trans. 47, 9617–9626.
Şenocak, A., Köksoy, B., Demirbaş, E., Basova, T.V., Durmuş, M., 2018c. Sens. Actuators B 267, 165–173.
Smith, A.M., Mohs, A.M., Nie, S., 2008. Nat. Nanotechnol. 4, 56–63.
Stachniuk, A., Fornal, E., 2016. Food Anal. Method 9, 1654–1665.
Terao, J., 2009. Flavonols; metabolism, bioavailability and health impacts. In: Fraga, C.G. (Ed.), Plant Phenolics and Human Health. Wiley and Sons Inc, Hoboken, pp. 185–196.
Wepasnick, K.A., Smith, B.A., Bitter, J.L., 2010. Anal. Bioanal. Chem. 396, 1003–1014.
Yao, L., Xiao, S., Dan, F., 2013. J. Chem. 2013 (697850-10).
Zhang, Y.K., Kua, J., McCammon, J.A., 2002. J. Am. Chem. Soc. 124, 10572–10577.
Zhou, Y., Wang, S., Zhang, Y., 2010. J. Phys. Chem. B. 114, 8817–8825.
Zhu, C., Yang, G., Li, H., Du, D., Lin, Y., 2015. Anal. Chem. 87, 230–249.